AGU PUBLICATIONS

Water Resources Research

RESEARCH ARTICLE
10.1002/2014WR016215

Key Points:
- Framework for Pareto-efficient environmental flow constraints on hydropeaking
- Compromise between grid-wide cost and subdaily hydrologic alteration
- Pareto-efficient constraints are found with cost increase below 2%

Correspondence to:
M. A. Olivares,
maroliva@ing.uchile.cl

Citation:
Olivares, M. A., J. Haas, R. Palma-Behnke, and C. Benavides (2015), A framework to identify Pareto-efficient subdaily environmental flow constraints on hydropower reservoirs using a grid-wide power dispatch model, *Water Resour. Res.*, *51*, 3664–3680, doi:10.1002/2014WR016215.

Received 30 JUL 2014
Accepted 7 APR 2015
Accepted article online 14 APR 2015
Published online 23 MAY 2015

A framework to identify Pareto-efficient subdaily environmental flow constraints on hydropower reservoirs using a grid-wide power dispatch model

Marcelo A. Olivares[1,2], Jannik Haas[1,2], Rodrigo Palma-Behnke[2], and Carlos Benavides[2]

[1]Department of Civil Engineering, Universidad de Chile, Santiago, Chile, [2]Energy Center, Department of Electrical Engineering, Universidad de Chile, Santiago, Chile

Abstract Hydrologic alteration due to hydropeaking reservoir operations is a main concern worldwide. Subdaily environmental flow constraints (ECs) on operations can be promising alternatives for mitigating negative impacts. However, those constraints reduce the flexibility of hydropower plants, potentially with higher costs for the power system. To study the economic and environmental efficiency of ECs, this work proposes a novel framework comprising four steps: (i) assessment of the current subdaily hydrologic alteration; (ii) formulation and implementation of a short-term, grid-wide hydrothermal coordination model; (iii) design of ECs in the form of maximum ramping rates (MRRs) and minimum flows (MIFs) for selected hydropower reservoirs; and (iv) identification of Pareto-efficient solutions in terms of grid-wide costs and the Richard-Baker flashiness index for subdaily hydrologic alteration (SDHA). The framework was applied to Chile's main power grid, assessing 25 EC cases, involving five MIFs and five MRRs. Each case was run for a dry, normal, and wet water year type. Three Pareto-efficient ECs are found, with remarkably small cost increase below 2% and a SDHA improvement between 28% and 90%. While the case involving the highest MIF worsens the flashiness of another basin, the other two have no negative effect on other basins and can be recommended for implementation.

1. Introduction

Hydropower plants typically compensate for short-term differences between power generation and demand through an operational scheme commonly known as *hydropeaking*. These plants usually supply energy at maximum capacity in peak hours, while they run at a low power output—or even shut down—during off-peak hours, with the consequent fluctuations in turbined flows. This operational pattern might be exacerbated under heavy penetration of fluctuating renewable energy technologies on system with large fraction of hydropower [*Haas et al.*, 2015; *Kern et al.*, 2014]. Short-term fluctuations in turbined flows can have negative impacts downstream of the plant's restitution point, potentially affecting the ecosystem and other human water uses. In fact, severe ecological consequences of hydropeaking have been documented in the literature. Reported impacts include a reduction of invertebrate biomass [*Moog*, 1993], stranding of juvenile individuals in anadromous fish species [*Saltveit et al.*, 2001; *Halleraker et al.*, 2003; *Tuhtan et al.*, 2012], negative impact on mobility and home range of juvenile Atlantic salmon [*Scruton et al.*, 2005], reduction in native species richness [*Vehanen et al.*, 2005], alteration of the hyporheic habitat [*Bruno et al.*, 2009], degraded fish habitat [*García et al.*, 2011], and alteration of the thermal regime [*Krause et al.*, 2005].

To date, the most widespread approach to address the issue of altered flows involves the use of the Indicators of Hydrologic Alteration (IHA) [*Richter et al.*, 1996]. However, the IHA approach relies on daily flow measures, which cannot capture the subdaily fluctuations associated with hydropeaking [*Baker et al.*, 2004]. Furthermore, *Bevelhimer et al.* [2015] found that metrics of subdaily hydrologic alteration are uncorrelated with the daily IHA. Some studies have extended the IHA approach by incipiently incorporating indicators of subdaily fluctuations [*Halleraker et al.*, 2007; *Meile et al.*, 2010]. Specific studies proposing indicators of subdaily hydrological alteration are relatively scarcer in literature. Notably, *Zimmerman et al.* [2010] presented a framework to study the impacts of hourly dam operations at a basin scale using four subdaily metrics: (i) Richards-Baker flashiness index [*Baker et al.*, 2004], (ii) number of reversals in flow [*The Nature Conservancy*, 2007], (iii) percentage of total flow [*Lundquist and Cayan*, 2002], and (iv) the coefficient of diel variation

[*McKinney et al*., 2001]. Similarly, *Bevelhimer et al*. [2015] used 13 subdaily statistics and found that the effects of hydropeaking are masked within daily indicators, which is in line with other recent studies [*Baker et al*., 2004; *Zimmerman et al*., 2010; *Haas et al*., 2014].

Unlike the case of IHA, where several studies have explored the ecological significance of the indicators [*Suen and Eheart*, 2006; *Yang et al*., 2008], to date no such study exists for subdaily indicators. However, studies have shown that natural subdaily flows are characterized by a quite steady regime with infrequent short-term fluctuations [*Zimmerman et al*., 2010; *Bevelhimer et al*., 2015]. Thus, under the assumption that the natural flow regime is best [*Poff et al*., 1997], larger values of subdaily indicators imply a less natural flow and hence a less desirable regime.

In response to the consequences of hydropeaking, several technical solutions have been proposed, among which operational constraints, in the form of minimum flows (MIF) and maximum ramping rates (MRR), are common. Since long ago, MIFs have been traditionally imposed to help preserving the natural habitat. However, nowadays it is broadly accepted that MIFs by themselves are insufficient to sustain a healthy river system [*Poff et al*., 1997; *Bunn and Arthington*, 2002; *Biggs et al*., 2005; *Poff and Zimmerman*, 2010]. Accordingly, MRRs, i.e., setting maximum allowable hourly flow changes, are becoming more popular [*Olivares*, 2008; *Pérez-Díaz et al*., 2012].

Several studies have explored the economic impact of environmental constraints (ECs), both in the form of MIF or MRR. For example, *Harpman* [1999] studied the regulation of hourly releases of Glen Canyon Dam's operation for one combination of MIF and up/down MRR, and obtained a decrease of 8% in the short-run revenue of the hydropower plant. *Pérez-Díaz and Wilhelmi* [2010] evaluated a set of MIF and MRR using a single plant, revenue-driven optimization model and found a linear relationship between MIF and costs, and a parabolic trend between MRR and costs. *Kotchen et al*. [2006] performed an expost economic analysis of relicensing two hydroelectric dams of Michigan, which changed from a peaking scheme to a run-of-river operation and found that the aggregated benefits from alternated uses doubled the producer's costs. *Kern et al*. [2012] used a revenue optimization model to assess the impact of deregulated power market schemes on the IHA induced at a daily level by a single hydropower plant. They found that real-time energy market participation offers great revenue improvements at the cost of little extra environmental alteration relative to the day-ahead only scheme, and that run-of-river operations are best at mimicking the natural regime, though at the expense of significant foregone revenues. *Shiau and Wu* [2013] used a simulation-optimization approach to derive multiobjective subdaily operation schemes for a single reservoir in Taiwan. Objectives included metrics for domestic water supply, hydropower generation, flood control, and environmental flows.

The aforementioned studies focus on the local—single plant to basin wide—economic impact of ECs. However, as every major hydropower reservoir is part of an intertied power system, evaluating the impact of ECs at a system level is crucial. A grid-wide approach has at least the following advantages. First, it ensures that the operational schemes obtained from the model are closer to those observed in reality, since hydropower reservoir operations are prescribed by grid-wide dispatch. Second, it suppresses the need to represent grid-wide operational drivers (e.g. power demands and fuel prices) using exogenous basin-scale proxies (e.g., electricity prices). Third, it allows observing cross effects among reservoirs located in different basins, as well as balancing the short-term fluctuations among all power plants in the grid. To the authors' best knowledge, this systemic approach for studying the impacts of ECs on hydropower is missing in the literature. Furthermore, the previous studies do not evaluate the effectiveness of EC in terms of improving indexes of hydrologic alteration.

This paper proposes a novel framework for designing and assessing the impact of cost-efficient, short-term operational constraints on hydropower reservoirs. This approach combines two main features: the use of a grid-wide operations model to represent hydropeaking in current and future scenarios, as opposed to basin-scale and historical records analysis, on which most previous work on subdaily hydrological alteration is based, and the identification of Pareto-efficient environmental constraints considering the trade-offs between the cost and the effectiveness measured in terms of an indicator of subdaily hydrologic alteration. The proposed framework is then applied to Chile's main grid, constraining the operations of a hydropower reservoir known for its severe hydrologic alteration. The results of the case study aim to assist policy makers to identify trade-offs between generation costs and environmental targets, particularly related to river flow

restoration. This approach could be included in future hydropower licensing and potential relicensing processes, in order to identify efficient ECs.

The paper is structured into four sections. The proposed framework is explained in section 2, while section 3 shows the case study. Section 4 presents the conclusions and future work.

2. Proposed Framework

The proposed framework to identify Pareto-efficient subdaily environmental flow constraints on hydropower reservoirs using a grid-wide power dispatch model is composed by four steps. The first step, a diagnostic, contrasts the current operations against the natural subdaily flow regime to explore the need for ECs. The second step formulates a centralized grid-wide optimization model to allow simulation of hydropower reservoir operations under selected water year scenarios. The third step deals with the design of the ECs to be implemented in the model, while the fourth aims to identify Pareto-efficient ECs and relevant trade-offs. This framework is flexible enough to adapt to different situations, including dispatch models or even power market structures, form of the operational constraints and which reservoirs those are imposed upon, and selection of indicators of subdaily hydrologic alteration. In any case, the framework requires a model capable to reproduce reservoir operations at the hourly level for the entire power grid.

2.1. Diagnostic

The first step consists of performing a diagnostic, comparing the current operation of the hydropower plants under study with the natural subdaily hydrologic regime. The key assumption here is that turbined flows determine to a great extent the instream flows downstream the restitution point. As mentioned above, natural flows at the subdaily scale are expected to be steady most of the time, with very infrequent events of large fluctuations [*Zimmerman et al*., 2010; *Bevelhimer et al*., 2015].

As many hydropower reservoirs operate in hydropeaking scheme, large changes of turbined flows can occur between consecutive hours. Consequently, to capture the phenomenon adequately, at least an hourly resolution for the natural and turbined flows needs to be used. Data availability for this level of detail can be scarce, particularly for the preintervention period. For young reservoirs, flow data from flow gauging stations close to the point of interest might be available prior to the date of construction. For older reservoirs, data from equivalent—still unaltered—basins might be used, coupled with several hydrologic methods to reconstruct the flow series and fill missing data. Information describing the current operation can easily be obtained from the power system operator, the plant operator, or existing flowmeters properly located.

The flow time series of the natural and current situation are then further processed to compute indexes of hydrologic alteration. As discussed earlier, using time series with hourly resolution is important to avoid time scales masking short-term peaking. Among the indices of subdaily hydrologic alteration (SDHA) proposed in the literature [*McKinney et al*., 2001; *Lundquist and Cayan*, 2002; *Baker et al*., 2004; *Haas et al*., 2014], the Richard-Baker (R-B) flashiness index [*Baker et al*., 2004] is one of the few that captures SDHA accounting for the sequence, magnitude, and amount of peaking events within a day. Equation (1) shows the R-B index as the sum of the differences between flows q_t of consecutive hours t and $t+1$, normalized by the total flow over time horizon T. This flashiness index allows summarizing the data of a whole day ($T = 24$ h) into one value. Consequently, for every day under study, there will be one value of the flashiness index describing the SDHA of the natural regime and current case.

$$\text{R-B Index} = \frac{0.5\sum_{t=1}^{T}(|q_{t+1}-q_t|+|q_t-q_{t-1}|)}{\sum_{t=1}^{T} q_t} \quad (1)$$

Analysis of several days results in a potentially large sample of flashiness indexes, which is then summarized by a duration curve. This way, every flashiness event gets associated with a probability of exceedance, which will allow determining how much more frequent a given event of hydrologic alteration becomes, and how much more severe an event gets for the same probability level. R-B index duration curves for the natural and altered regimes are then compared. A significant difference between both would call for ECs to help keeping the hydrologic alteration within acceptable levels. This diagnostic phase allows identifying which hydropower reservoirs are critical in terms of SDHA.

Table 1. Nomenclature of the Model

Name	Units	Description
Indexes		
g,i		Index of generators, between 1 and G
l		Index of transmission lines, between 1 and L
t		Index of time steps, between 1 and T
s		Index of hydrologic scenario of future cost function, between 1 and S
n		Index of the piecewise linear segment of the power loss approximation, between 1 and N
Sets		
$\mathbb{L}$		Set of transmission lines
$\mathbb{L}_b$		Subset of transmission lines that connect with bus b
$\mathbb{G}$		Set of power plant
$\mathbb{G}_T$		Subset of thermal and renewable power plants
$\mathbb{G}_H$		Subset of hydropower plants
$\mathbb{G}_{H,}$		Subset of hydropower plants with reservoirs
$\mathbb{G}_b$		Subset of power plants that connect with bus b
$\mathbb{U}_g$		Set of hydropower plants that are immediately upstream of hydropower plant g
$\mathbb{T}$		Set of time steps
|B		Set of buses
Variables		
$B_{g,t}$		Binary decision of generator g being off/on during time step t
$P_{g,t}$	MW	Decision of amount of power to be generated by generator g during time step t
$UE_{b,t}$	MW	Decision of amount of unserved energy at bus b during time step t
$R_{l,t}$	MW	Transmission losses at line l during time step t
$F_{l,t}$	MW	Decision of amount of power to be imported through line l during time step t
$\theta_{n,t}$	MW	Piecewise linear segment n of the approximation of power losses during time step t
$V_{g,t}$	10^3 m^3	Stored volume by hydropower plant g during time step t
$Q_{g,t}$	m^3/s	Turbined water by hydropower plant g during time step t
$QS_{g,t}$	m^3/s	Spilled water by hydropower plant g during time step t
$QF_{g,t}$	m^3/s	Fictitious inflows of hydropower plant g during time step t
FCF_s	USD	Value of future cost function of hydrologic scenario s
Inputs		
$QA_{g,t}$	m^3/s	Natural inflows to hydro power plant g during time step t
Q_g^{min}, Q_g^{max}	m^3/s	Minimum/maximum turbined flow of hydropower plant g
QS_g^{min}, QS_g^{max}	m^3/s	Minimum/maximum spilled flow of hydropower plant g
V_g^{min}, V_g^{max}	10^3 m^3	Minimum/maximum volume of reservoir of hydropower plant g
(QT_g^{min})	$(P^{min})_g, (P^{max})_g$	Minimum/maximum power output of power plant *g*
MIF_g	m^3/s	Minimum turbined flow
MRR_g	m^3/s/h	Maximum ramping rate
Δ t	h	Duration of time step t
c_g	USD/MWh	Operation cost of generator g
c_{UE}	USD/MWh	Penalization for unserved energy
η_g	MW/(m^3/s)	Water-power yield of hydropower plant g
$\alpha_{k,s,g}$	USD/(10^3 m^3)	Benders cut slope of future cost function of iteration k and hydrologic scenario s for hydropower reservoir g
$\beta_{s,k}$	USD	Benders cut *y* intercept of future cost function of iteration k and hydrologic scenario s
$D_{b,t}$	MW	Demand at bus b during time step t
$tMin_g^{on}$, $tMin_g^{off}$	H	Minimum on/off time of power plant g expressed in hours
$bMin_{g,t}^{on}$, $bMin_{g,t}^{off}$		Minimum on/off time steps of power plant g measured since step t
$bfMin_g^{on}$, $bfMin_g^{off}$		Time steps from which min on/off time constraint of generator g exceeds the time horizon
γ_n		Slope of the nth piecewise linear segment of the approximation of power losses
γ_n^{max}	MW	Upper bound of the sth piecewise linear segment of the approximation of power losses

2.2. Power System Modeling Tool

To evaluate the impact of ECs in terms of both costs and operational patterns, a predictive tool is needed. As hydropower plants are usually part of an intertied grid, this tool should consider the whole system in order to be able to detect cross effects between the new (restricted) operation of the plant and the remaining power generators. In this paper, a classical hydrothermal optimization model is formulated from the point of view of a centralized system operator. The main decision variables in the model are the hourly power produced by each plant within the time horizon and the stored water volume at the end of the planning horizon for each reservoir. The model then minimizes the total cost, including operational cost, opportunity cost of water, and the cost of unserved load, subject to technical, hydropower, water balance, and power flow constraints. Table 1 provides a notation list of the indexes, variables, and inputs of the model. In the following paragraphs, the model will be explained with further detail.

2.2.1. Objective Function

The objective function (equation (2)) minimizes the sum of three cost components: (i) operational costs of the set G_T of thermal and renewable power plants g over time horizon T, (ii) the opportunity cost of end-of-horizon stored water over water inflow scenarios S, and (iii) the cost of unserved load at the buses B of the grid over time T, where c_g is the variable cost of generator g, $P_{g,t}$ the power generated by g during time step t, FCF_s the future cost function of hydrologic scenario s, c_{UE} the penalty of unserved load, and $UE_{b,t}$ the amount of unserved energy at bus b during period t. The shown formulation allows using hourly (Δ t = 1), variable multihourly (Δ t > 1) or variable subhourly (Δ t < 1) time steps or time blocks.

$$Min\ Z = \sum_{t,g}^{T,G_T} c_g\ \boldsymbol{P_{g,t}} \Delta t + \sum_{s}^{S} \frac{1}{S} \boldsymbol{FCF_s} + \sum_{t,b}^{T,B} c_{UE} \boldsymbol{UE_{b,t}}\ \Delta t. \tag{2}$$

2.2.2. Technical Constraints

Equations (3–5) show technical constraints on power plants. The range of the power output of each plant is limited by the minimum P_g^{min} and maximum capacity P_g^{max}, when turned on, i.e., $B_{g,t}$=1 (equation (3)). Equation (4) assures a power plant is turned on during a minimum amount of hours $tMin_g^{on}$. The difference between this time $tMin_g^{on}$ and the parameter $bMin_{g,t}^{on}$ is that the latter is the conversion between hours and time steps. If the time resolution is constant and equal to 1 h, both parameters are the same. Equation (5) has the same purpose as (4), but is used if $tMin_g^{on}$ cannot be further met, because the optimization is reaching the final hours of the planning horizon. In other words, an amount of $bfMin_g^{on}$ time steps before the end of the time horizon, equation (5) is used instead of equation (4). Similar constraints are used for the minimum time off, but for simplicity not shown.

$$B_{g,t}\ P_g^{min} \le\ P_{g,t} \le B_{g,t} P_g^{max},\ \forall\ t, g\ \epsilon\ \mathbb{G}, \tag{3}$$

$$\sum_{ta=t}^{t+bMin_{g,t}^{on}-1} \Delta_{ta} B_{g,ta} \ge tMin_g^{on} (B_{g,t} - B_{g,t-1})$$
$$\text{when}\ \ 1 \le t \le T - bfMin_g^{on},\ \forall t, g\ \epsilon\ \mathbb{G}, \tag{4}$$

$$\sum_{ta=t}^{T} \Delta\, tB_{g,ta} \ge \left(\sum_{ta=t}^{T} \Delta t \right) (B_{g,t} - B_{g,t-1})$$
$$\text{when}\ \ t > T - bfMin_g^{on},\ \forall t, g\ \epsilon\ \mathbb{G}. \tag{5}$$

2.2.3. Hydro Constraints

Equations (6) and (7) apply to all hydropower plants $\mathbb{G}_H$, while equations (8) and (9) apply to hydropower plants with reservoirs $\mathbb{G}_{H_r}$ only. An important parameter is the yield η_g between water and power, which depends on several phenomena, such as: head of the reservoir, aggregated efficiency curves (or hill curves) of turbines, head losses in water conduction, and water level over the outlet. Knowing the yield allows equation (6) to relate turbined flow $Q_{g,t}$ with power $P_{g,t}$, while equation (7) checks the turbined flow of each plant is above the technical minimum Q_g^{min} and below its maximum Q_g^{max}, when turned on. Equations (8) and (9) verify the stored volume $V_{g,t}$ and the spilled water $QS_{g,t}$ are within their feasible range V_g^{min} to V_g^{max} and QS_g^{min} to QS_g^{max}, respectively.

$$P_{g,t} = \eta_g Q_{g,t}\ \forall\ t, g\ \epsilon\ \mathbb{G}_H, \tag{6}$$

$$B_{g,t}\ Q_g^{min} \le Q_{g,t} \le B_{g,t} Q_g^{max}\ ,\ \forall\ t, g\ \epsilon\ \mathbb{G}_H, \tag{7}$$

$$V_g^{min}\ \le\ V_{g,t} \le V_g^{max}\ ,\ \forall\ t, g\ \epsilon\ \mathbb{G}_{H_r}, \tag{8}$$

$$QS_g^{min} \le\ QS_{g,t} \le QS_g^{max}\ ,\ \forall\ t, g\ \epsilon\ \mathbb{G}_{H_r}. \tag{9}$$

2.2.4. Water Balance

Equation (10) makes sure the water balance of each hydropower plant is met. It takes into account the variation of stored water, inflows $QA_{g,t}$, turbined flow, spilled water, fictitious inflows $QF_{g,t}$, and turbined and

spilled water from hydroplants located upstream $\mathbb{U}_g$. For hydropower plants without a reservoir, the change of stored water is equal to zero. The fictitious inflows are auxiliary variables to help the convergence of the model. These are strongly penalized in the objective function, although this is not shown in equation (2), so that in the optimal solution they are equal to zero.

$$\frac{V_{g,t}-V_{g,t-1}}{3.6\Delta_t}=QF_{g,t}-Q_{g,t}-QS_{g,t}+QA_{g,t}+\sum_{u\ \epsilon\ \mathbb{U}_g}Q_{u,t}+\sum_{u\ \epsilon\ \mathbb{U}_g}QS_{u,t},\ \ \forall\ t,g\ \epsilon\ \mathbb{G}_H. \tag{10}$$

2.2.5. Power Flow and Line Losses

The model considers the transmission grid $\mathbb{L}$. The buses b of the system are interconnected by transmission lines l, on which the flow is calculated using a direct current flux model with losses. The main equation of this model is the nodal power balance as shown in equation (11), while the remaining equations of the power flow model can be consulted in *Stott et al.* [2009]. The generated power considers the sum of the power output of all generators $\mathbb{G}_b$ (thermal, renewable, and hydro) connected to a given bus; the unserved energy is an auxiliary variable to help the convergence of the model and is heavily penalized in the objective function; imported/exported power fluxes $F_{l,t}$ are all the flows from/to neighboring buses $\mathbb{L}_b$; and the power losses $R_{l,t}$ represent to the losses inherent to transmission. The right-hand term is the demand $D_{b,t}$ of a given bus.

The power losses are represented by a quadratic function, $R_{l,t}=\mathrm{F_{l,t}}^2/\mathrm{x_l}$, where $\mathrm{x_l}$ is the reactance of the line l, which is approximated by n piecewise linear segments [*Dos Santos and Diniz*, 2011]. This approximation is shown in equations (12–14), where $\theta_{n,t}$ is the *n*th piecewise linear segment and γ_n is the slope of the *n*th piecewise linear segment. Particularly, equation (12) refers to the power flow as function of the piecewise approximation, while equation (13) computes the losses and equation (14) sets the lower and upper bound of each segment's power loss in that approximation.

$$\sum_{g\ \epsilon\ \mathbb{G}_b}P_{g,t}+UE_{b,t}+\sum_{l\epsilon\ \mathbb{L}_b}F_{l,t}+\sum_{l\epsilon\ \mathbb{L}_b}R_{l,t}=D_{b,t},\ \ \forall t,b, \tag{11}$$

$$F_{l,t}=\sum_{n\in N_s}\theta_{n,t},\ \ \forall t,l, \tag{12}$$

$$R_{l,t}=\sum_{n\ \in\ N_s}\gamma_n\theta_{n,t},\ \ \forall t,l, \tag{13}$$

$$0\le\theta_{n,t}\le\theta_n^{max}\ \ ,\forall n. \tag{14}$$

2.2.6. Opportunity Cost of Water

When storage for hydrogeneration is large within a system, the long-term opportunity cost of water becomes relevant and as so it must be included in the short-term operation planning. One alternative to estimate this cost is using a model based on Benders cuts, also known as stochastic dual dynamic programming or SDDP, which calculates the cost of displaced thermal generation [*Pereira and Pinto*, 1991]. This method is particularly advantageous to confront the computational burden of multireservoir systems. It alternates between forward and backward iterations until reaching a convergence criterion, and can consider the stochasticity of inflows for each scenario that needs to be evaluated. This method generates a multidimensional cost function composed by multiple slopes $\alpha_{k,s,g}$ (of iteration k of inflow-scenario s for hydropower reservoir g), and *y* intercept $\beta_{s,k}$ (of iteration k and inflow-scenario s), for the stored volume vector of the reservoirs at the end of the time horizon $V_{g,\bar{T}}$. Once the cost function is known, it is used as an input to the present short-term optimization, where equation (15) makes sure to minimize the resulting cost as function by deciding $V_{g,\bar{T}}$.

$$FCF_s\ge\beta_{s,k}+\sum_{g\,\epsilon\,\mathbb{G}_{H_r}}\alpha_{k,g,s}V_{g,\bar{T}},\forall s,k. \tag{15}$$

2.2.7. Design of Environmental Constraints

Environmental constraints are to be designed and added to the aforementioned model. Here minimum flows are defined as minimum turbined flows MIF_g (equation (16)), which must be met regardless of the on-off state of the plant. In other words, this condition is more stringent than equation (7). On the other hand, maximum ramping rates MRR_g are defined as maximum absolute difference between the current turbined

flow and that of the previous time step. This is shown in equations (17) and (18) structured as up-ramp and down-ramp constraints.

$$Q_{g,t} \geq MIF_g \ \forall \ t, g \ \epsilon \ \mathbb{G}_{H_r}, \tag{16}$$

$$Q_{g,t} - Q_{g,t-1} \leq MRR_g \ , \ \forall \ t, g \ \epsilon \ \mathbb{G}_{H_r}, \tag{17}$$

$$Q_{g,t} - Q_{g,t-1} \geq -MRR_g \ , \ \forall \ t, g \ \epsilon \ \mathbb{G}_{H_r}. \tag{18}$$

In addition to the structure of the constraints, numerical values for these must be defined. To move toward the restoration of natural flow regime, the unaltered flow series can be analyzed to identify ranges of MIF and MRR that are natural. This should originate a set of combinations of MIFs and MRRs to explore.

2.2.8. Pareto-Efficiency of Operational Constraints

From the optimization model, relevant results are the weekly cost and hourly operation of the system. The goal of this section is to find one—or a set of—ECs that are effective in achieving environmental goals at the lowest possible costs. The environmental goals herein defined as improvements in the flashiness index between the base case and the EC under evaluation. Thus, the operation of the power plants needs to be translated into flows followed by computing the flashiness index as show in section 2.1. On the other hand, the cost refers to the systemic cost increase induced by the EC. Thus, the impact is two dimensional as the environmental performance criterion is difficult to translate into monetary units. Consequently, the results of the analyzed cases, improvement in flashiness index and systemic cost increase, can be compared on a biaxial plot on which the Pareto-front can be identified. Finally, it is important to verify that these efficient EC do not have a negative impact on flashiness indexes downstream of other reservoirs of the system. For this task, it is recommended to compare the flashiness of the base case with the EC-cases for every relevant reservoir of the system.

3. Case Study

The proposed framework is applied to the main power system in Chile: the Central Interconnected System (SIC). The Chilean SIC is a hydrothermal power system, i.e., it is mainly composed by thermal (50%) and hydro (45%) power plants; the remaining generators are small renewables. The system is structured as a pool with audited costs, in which operational decisions are made by an independent system operator (ISO). The ISO splits the problem into two major time horizons. It first computes the long-term opportunity cost of water, using a stochastic optimization model based on Benders [*Pereira and Pinto*, 1991], for about 50 historical flow scenarios. Stochasticity is associated with the inflows to the hydropower plants and reservoirs of the whole system in each scenario. Afterwards, these results are used to determine the hourly operation of the system within a week. To be as close as possible to the current practices of Chile's ISO, environmental flow constraints were added to a model which replicates its current short-term dispatch tool.

Regulation in Chile stipulates that the ISO's orders are compulsory and independent of each company's energy and power supply contracts. As a result, transfers are often made between generators to enable them to meet their commercial obligations, which are valued at the hourly locational marginal cost (spot price). The segregation between dispatch and contracts allows the system to minimize short-run total production cost.

The four steps of the proposed framework are now applied to the case study as follows. Although the ECs are applied to a single power plant, the model still represents the operations of the entire grid.

3.1. Diagnostic

In Chile's SIC, most of the hydropower comes from the south, whereas the load centers are located in central Chile, as shown in Figure 1. Nine reservoirs regulate the flows of the main rivers, with power capacity ranging between 95 and 690 MW, and storage capacity between weekly and yearly regulation. These projects, built prior to 2005 in which a bill for minimum flows was passed [*Ministry of Public Works of Chile (MOP)*, 2005], have no obligations regarding ECs (although some agreed to a small MIF voluntarily).

As most of the load-following operation is done by hydropower plants, significant fluctuations downstream of the restitution point of turbined flows are induced. In this study, attention is focused on hydropower

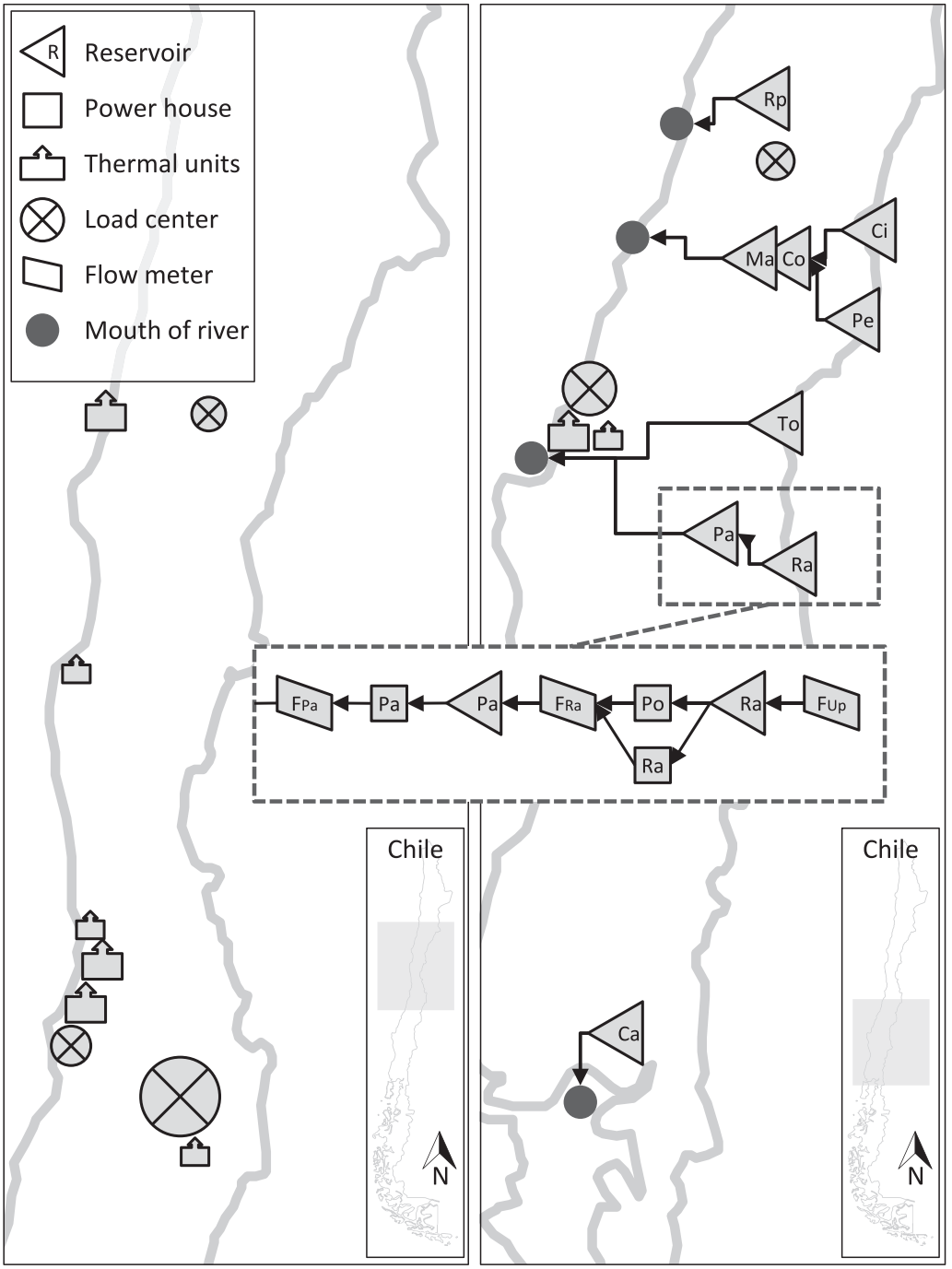

Figure 1. Simplified schematic of SIC and zone of study, showing the location of aggregated thermal power plants, hydropower reservoirs, and main load centers (abbreviation of reservoirs: Rp, Rapel; Ma, Machicura; Co, Colbún; Ci, Cipreses; Pe, Pehuenche; To, El Toro; Pa, Pangue; Ra, Ralco; and Ca, Canutillar).

reservoirs Pangue (465 MW, 70 Mm^3), El Toro (450 MW, 5590 Mm^3), and Machicura (95 MW, 20 Mm^3), because those are the most downstream reservoir of their basin, thus controlling the regime of the remaining river. Because Pangue is known for its severe hydropeaking, affecting one of the main rivers in central Chile, this diagnostic will focus on that reservoir. Nevertheless, the proposed framework can consider a diagnostic performed for every reservoir in the grid.

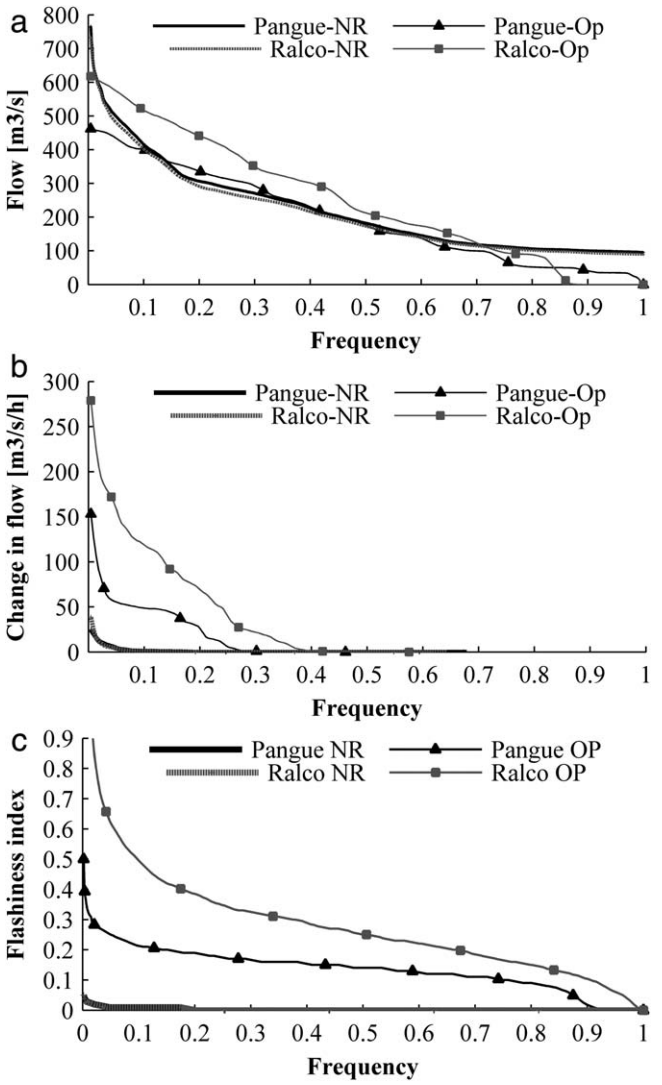

Figure 2. (a) Flow rate, (b) change in flow rate, and (c) R-B flashiness index of Pangue and Ralco for their natural regime (NR) and operation (OP) between 2010 and 2011.

Pangue receives the turbined flows from two plants, Ralco ("Ra") and Polcura ("Po"). Pangue releases an environmental flow of 50 m^3/s through the turbines. As a reference, the average river flow is 290 m^3/s. However, during dry periods, the output has been lowered to its technical minimum of 35 m^3/s or even shut down as it can be observed in Figure 2a. Several flowmeters are located along the system and their data can be accessed publicly [*National Directorate for Water of Chile*, 2013].

To illustrate the fluctuating operation of the Ralco-Pangue system, the operation based on hourly data of 2010–2011 is compared to the reconstructed natural regime for the same period. For this purpose, data from flow gauges below Pangue F_{Pa}, below Ralco F_{Ra}, and above Ralco F_{Up} are used [*National Directorate for Water of Chile*, 2013]. The information of those gauges is quite complete for the aforementioned period, with about 8% of missing data. The first two gauges record the total instream flow immediately downstream of the restitution point of Pangue and Ralco, respectively. The third, on the other hand, measures the unintervened basin upstream of Ralco, and is used to reconstruct the natural flow regime of Pangue and Ralco at their current restitution point.

For the period 2010–2011, duration curves of flow rate (m^3/s), hourly change in flow ($m^3/s/h$) and resulting R-B flashiness index (by using equation (1)) are plotted in Figure 2, for both the natural and altered flow regimes. It becomes clear that: (i) the natural regime of Pangue and Ralco is very similar in terms of flow rate, change of flow rate and flashiness index; (ii) the natural regime shows higher flow rates during a few extreme events; (iii) the smallest flows observed under the natural regime (about 100 m^3/s) are much larger than those for the intervened situation (between 0 and 50 m^3/s); (iii) the natural regime is characterized by small hourly changes in flow rates, with changes below 40 $m^3/s/h$ in the worst case; whereas operations of Pangue and Ralco induce flow rate changes up to 150 and 270 $m^3/s/h$, respectively; (iv) the natural river's flashiness is smaller than 0.03 (R-B index very close to the x axis), except for flooding events that reach an index of 0.05, occurring about 5 days per year. In summary, both Ralco's and Pangue's operations are far more fluctuating than the natural regime. The median value of the flashiness index of the natural regime is always exceeded. This motivates to explore how different operational constraints on Pangue, the downstream reservoir, help restoration toward the natural regime.

3.2. Power System Modeling Tool

3.2.1. Details of Inputs

Most of the data were obtained from Chile's ISO [*Power System Operator of Chile (CDEC)*, 2013], such as the minimum and maximum capacity of the power plants, hydraulic connectivity, minimum and maximum amount of turbined flow and spilled water, minimum and maximum stored volume in water reservoirs, hydraulic connectivity, penalty of unserved energy, penalty for fictitious inflows, and parameters related to the transmission grid. Minimum on and off times are inferred based on historic data of the ISO. A 1 h time step was used in the study.

Actual demand values of 2011–2013 were used. To account for seasonal variability of load, one typical week per month, defined as the week that minimizes the deviation regarding the remaining weeks of the set, was chosen from that record.

The future cost functions for those selected weeks were used as inputs (to equation (15)). The water-to-power yield is assumed to be constant for run-of-river plants. The yield for reservoirs is updated only once at the beginning of every week as function of the head of stored water as the small variations in the reservoir level that occur within a week have only little effect on the power yield value.

Outages and downtimes, due to failures or maintenance were not considered. The variable operation cost of thermal plants as of April 2013 is used and considered as constant under all scenarios [*National Energy Commission of Chile (CNE)*, 2013].

3.2.2. Scenario Definition

To study the behavior of the hydropower reservoirs under different water year types, three hydrologic scenarios are defined: dry, normal, and wet, with a probability of exceedance of annual flows of 20%, 50%, and 90%, respectively. The choice of those scenarios is based on data availability and the need to test the sensitivity of results in extreme cases. In order to consider time and spatial correlation of flows, three real years were used, chosen among the approximately 50 years of system-wide flow records. For each week of each hydrologic scenario, the initial volume of reservoirs was defined as the median value of the historic records.

3.3. Design of Environmental Constraints

In this section, values for MIF and MRR constraints are defined. MIF values are defined from the weekly median natural flows at Pangue, available from the records of the system operator [*Power System Operator of Chile (CDEC)*, 2013] for the years 1960–2000. The median flow per month is identified and five levels are defined as percentages of those monthly flows: 20, 30, 40, and 50% (plus the unrestricted case). Larger MIFs were not considered as they could be infeasible during dry years.

Hourly records of the natural flow regime at Pangue are available only for the last decade [*National Directorate for Water of Chile*, 2013] at the flowmeter F_{Up}. The drainage area at the location of the flowmeter and at the restitution point of Pangue is similar (5100 and 5400 km^2, respectively). Hence, the flow variations measured at F_{Up} are assumed to be representative for the natural flow regime of Pangue, in relative terms. From that record a dry, normal and wet year is identified and the flow changes between consecutive hours are calculated. Finally, MRR are defined as relative flow variations per hour of 6, 12, 14, and 28% (plus the unrestricted case) respect to the monthly median. These cases of MRR have probabilities of exceedance in the natural regime of 0.01%, 0.05%, 0.1%, and 0.5%, corresponding to extremely unlikely events. Exploring more restrictive cases would result in very small and similar flow variations, which would not contribute to exploring a significant range of constraints within the power system. This information is summarized in Table 2.

Table 2. Definition of Operational Constraints

Constraint		Criteria	Constraint		Criteria
Minimum flow (MIF)	MIF1	Current MIF	Maximum ramping rate (MRR)	MRR1	Unconstrained
	MIF2	20% of monthly median flow		MRR2	28% of monthly median flow
	MIF3	30% of monthly median flow		MRR3	14% of monthly median flow
	MIF4	40% of monthly median flow		MRR4	12% of monthly median flow
	MIF5	50% of monthly median flow		MRR5	6% of monthly median flow

Table 3. Value of MIF (m^3/s) and MRR ($m^3/s/h$)

Month	MIF1	MIF2	MIF3	MIF4	MIF5	MRR1	MRR2	MRR3	MRR4	MRR5
Jan	0	29	43	57	71	-	40	20	17	9
Feb	0	20	29	39	49	-	27	14	12	6
Mar	0	16	24	32	40	-	22	11	10	5
Apr	0	15	23	30	38	-	21	11	9	5
May	0	24	36	49	61	-	34	17	15	7
Jun	0	68	102	136	169	-	95	47	41	20
Jul	0	71	106	142	177	-	99	50	43	21
Aug	0	64	97	129	161	-	90	45	39	19
Sep	0	73	110	147	183	-	103	51	44	22
Oct	0	89	134	179	223	-	125	63	54	27
Nov	0	88	132	177	221	-	124	62	53	26
Dec	0	53	80	106	133	-	74	37	32	16

The percentages in Table 2 are then translated into the values per month as shown in Table 3, which are then used as inputs for the optimization model. However, if the resulting value of MIF in a given month is below the current MIF, the latter is adopted.

The above single-type constraints are combined, forming a total of 25 cases. Each of these cases is named such that, for example, Q1R3 represents the combination of MIF1 and MRR3, and so on.

3.4. Pareto-Efficiency of Operation Constraints

After running the described optimization problem for each of the 25 cases, the prescribed operation for the whole power system in study is known. The water year type defined earlier allow performing a scenario analysis. After computing the flashiness index, the effect of ECs on hydrologic alteration can be illustrated, followed by the cost analysis of each EC. With this information, Pareto-efficient solutions can be identified. For those, the cross effects between the constrained operation of Pangue and other hydropower plants will be analyzed.

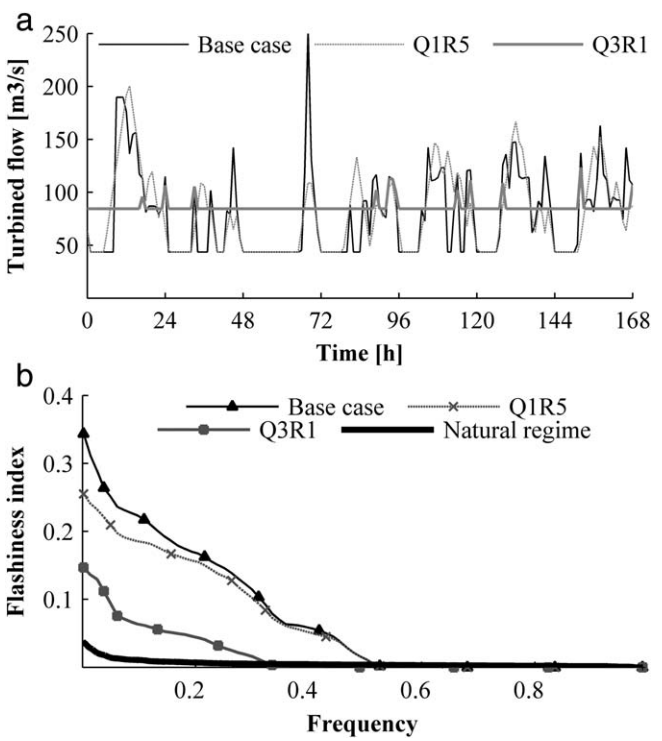

Figure 3. Example of two EC, Q3R1 and Q1R5, and their impact (a) on operation of Pangue and (b) on R-B flashiness index downstream of Pangue.

3.4.1. Effect of ECs on Pangue's Operation

As it can be seen on the example in Figure 3a, under current operation Pangue exhibits at least one major power spike during each day, sometimes even up to four. Two cases are chosen to illustrate the effect of ECs: a pure MRR (Q1R5), and a pure MIF (Q3R1). As expected, under pure MRR the ability of the power plant to quickly change its output is limited. Nevertheless, it can still follow price signals in a restricted way. On the other hand, MIF impacts the operation in two ways: a higher lower bound reduces the allowable operational range; and water allocated to MIF cannot be allocated for hydropeaking. Particularly for the shown timeframe, the pure MIF constraint is very effective in generating a steadier water output of Pangue.

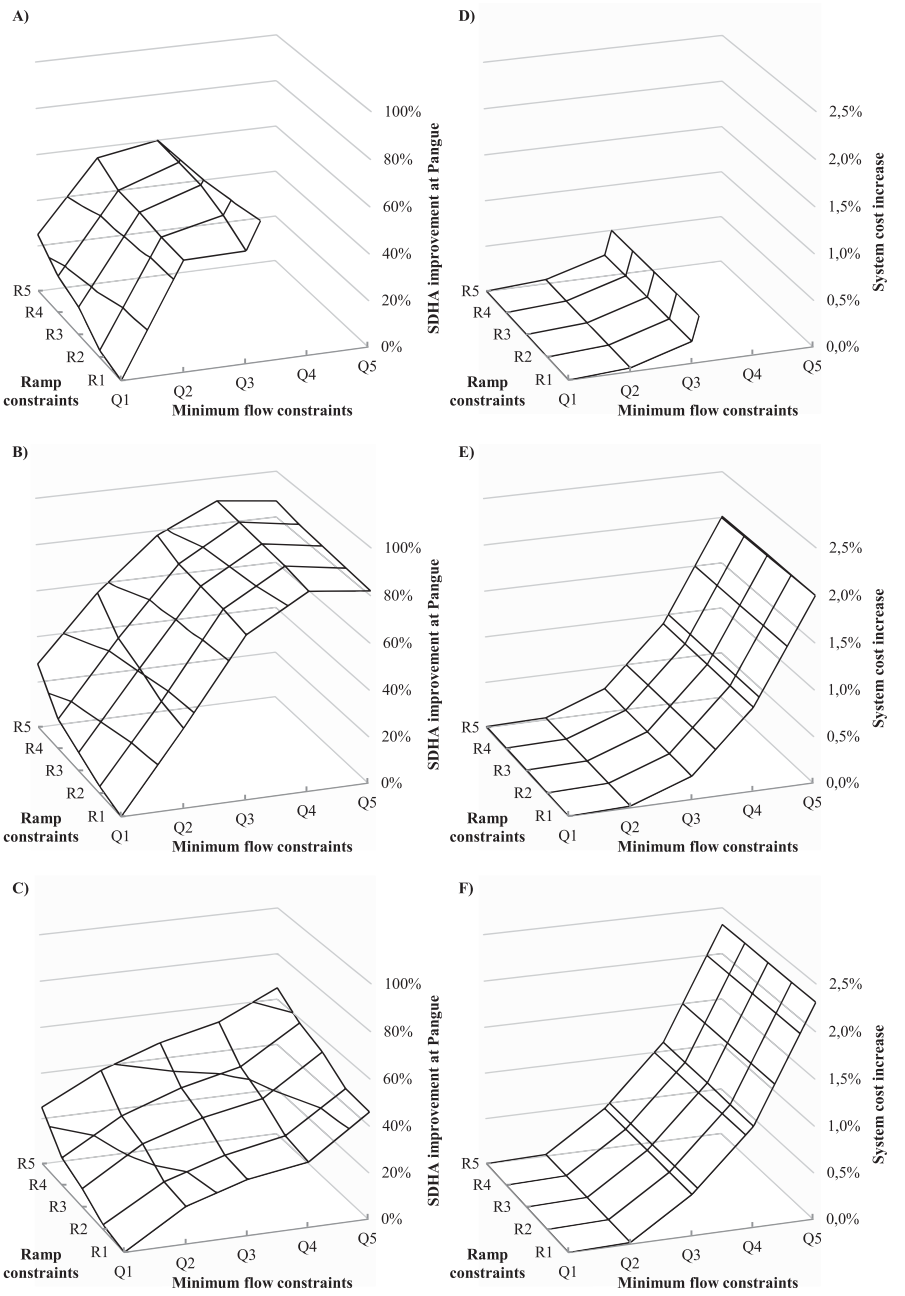

Figure 4. Improvement of the relative flashiness index downstream of Pangue's power plant for a (a) dry, (b) normal, and (c) wet year, and total (operational) system cost increase for a (d) dry, (e) normal, and (f) wet year, due to ECs.

3.4.2. Effect of EC on Hydrologic Alteration

In this step the flashiness index is computed and the sample of daily values is plotted in duration curves. These curves summarize the operation of the selected weeks in the year, from which the impact of different EC can be compared. As example in Figure 3b, two extreme cases are illustrated: the very fluctuating current operation of Pangue (base case) and the much steadier natural regime. Between those extremes, the results for two ECs are drawn. It can be observed how constraint Q1R5 helps decreasing extreme events (upper left part of the plot) by a 30% approximately (for example the maximum value of the R-B index, 0.35, is reduced to 0.25), but events above a probability of exceedance of 0.15 are not smoothed significantly. Constraint Q3R1, on the other hand, does a better job moving Pangue's release pattern closer to the natural regime.

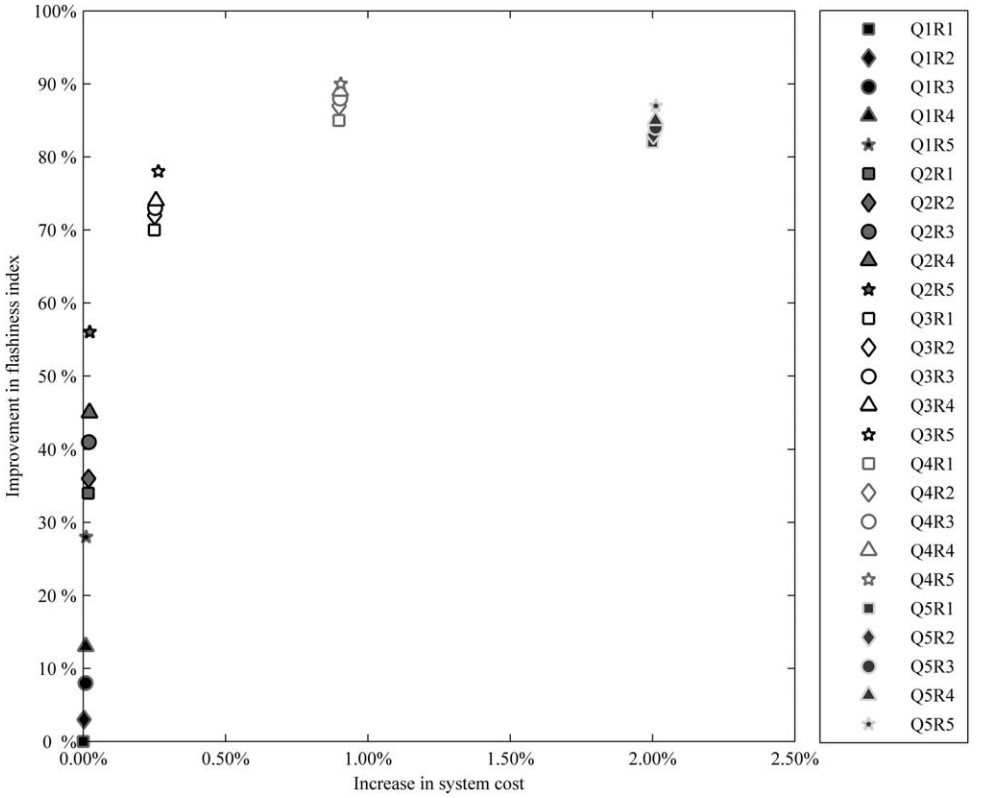

Figure 5. Trade-off curve between relative system cost increase and relative improvement in R-B flashiness index at Pangue due to ECs.

For ease of comparison between all 25 EC cases, the SDHA improvement is defined as the difference between the average daily flashiness index of each case and the base case average. A more sophisticated analysis, involving for example a range of variability approach [*Richter et al*., 1997], was impractical as the natural subdaily variability was almost negligible. The SDHA improvement is shown in Figures 4a–4c for a dry, normal, and wet water year type, respectively. In general, ECs reduce the flashiness index for all cases and water year type. However, MIF tend to achieve better results than MRR alone.

Regarding the effect of water year type, during a normal year, major improvements in the index, up to (a relative) 100%, are achieved for MIF constraints as stringent as MIF4, while more stringent constraints do

Table 4. Relative SDHA Improvement at Pangue (%) and Relative System Cost Increase of EC (%) Under Dry, Normal, and Wet Years[a]

	Dry Years					Normal Years					Wet Years				
	MIF1	MIF 2	MIF 3	MIF 4	MIF 5	MIF 1	MIF 2	MIF 3	MIF 4	MIF 5	MIF 1	MIF 2	MIF 3	MIF 4	MIF 5
SDHA Improvement															
MRR1	0.00	0.47	0.48	N/A	N/A	0.00	0.35	0.70	0.87	0.83	0.00	0.16	0.24	0.29	0.46
MRR2	0.05	0.47	0.54	N/A	N/A	0.02	0.36	0.71	0.88	0.83	0.00	0.17	0.25	0.30	0.47
MRR3	0.12	0.49	0.58	N/A	N/A	0.08	0.41	0.73	0.88	0.84	0.08	0.24	0.32	0.37	0.54
MRR4	0.16	0.49	0.59	N/A	N/A	0.13	0.45	0.74	0.89	0.84	0.12	0.27	0.36	0.42	0.58
MRR5	0.25	0.55	0.64	N/A	N/A	0.28	0.56	0.78	0.90	0.87	0.25	0.38	0.47	0.53	0.65
Cost Increase															
MRR1	0.00	0.04	0.24	N/A	N/A	0.00	0.02	0.25	0.90	2.00	0.00	0.02	0.44	1.08	2.31
MRR2	0.00	0.04	0.24	N/A	N/A	0.00	0.02	0.25	0.90	2.00	0.00	0.02	0.44	1.08	2.31
MRR3	0.00	0.04	0.24	N/A	N/A	0.01	0.02	0.25	0.90	2.01	0.00	0.02	0.44	1.10	2.31
MRR4	0.00	0.04	0.24	N/A	N/A	0.01	0.02	0.25	0.90	2.01	0.00	0.02	0.44	1.10	2.32
MRR5	0.00	0.05	0.24	N/A	N/A	0.01	0.02	0.26	0.91	2.01	0.00	0.02	0.44	1.10	2.32

[a]During dry years, MIF4 and MIF5 are not feasible. Thus, there are no results for these cases (N/A).

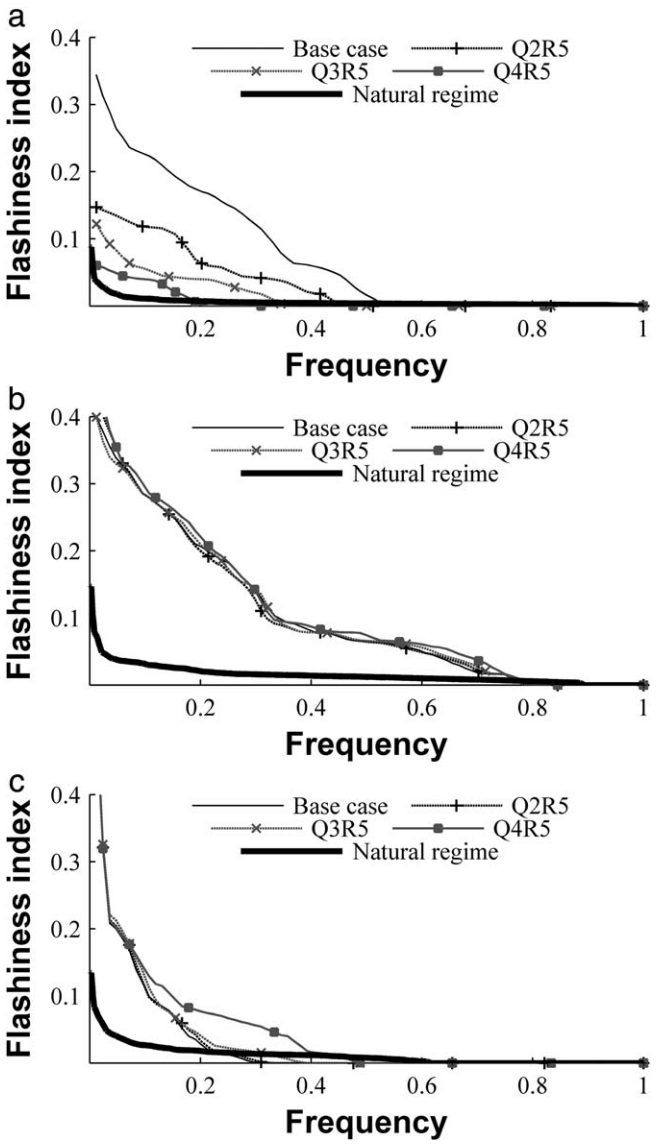

Figure 6. Natural regime, base case and impact of the three Pareto-efficient ECs (Q2R5, Q3R5, Q4R5) on the R-B flashiness index for reservoirs (a) Pangue, (b) Machicura, and (c) El Toro.

not result in significant improvement of river's flashiness. Even small MIFs help to establish a constant flow in the river, reducing available water for peaking. If MRRs are added, then the magnitude of those peaks is further reduced. In dry years the trend is similar; especially the set of constraints involving MIF2 is very effective in improving the mean of the flashiness index. It should be noted that the cases associated with MIF4 and MIF5 of the dry year cannot be met, due to the insufficient amount of water available. In these cases, to avoid infeasibilities, dynamic MIF constraints, as function of the monthly forecasted inflows, should be studied in the future. During wet years, though, the behavior is different; the constraints appear to have a linear and smaller effect on the flashiness index. Here the most restrictive case only reaches an enhancement of 75% approximately. This can be explained because, due to the larger inflows: Pangue shows a steadier operation at high output levels even in unregulated cases. In summary, when dry, normal and wet years are compared to each other, it becomes clear that especially during the former two, ECs make a great difference on flashiness indexes. Although the effect during wet years is much smaller, it still contributes toward to goal of achieving an environmentally friendlier flow.

3.4.3. Effect of ECs on System Costs

Besides the impact of the ECs on the flashiness index downstream of Pangue, it is relevant to know how much these ECs will cost system wide. Figures 4d–4f shows the cost increase for dry, normal and wet years. In all cases, the costs of ECs are below 2.5% of the total system cost, or about 30 million USD per year. When comparing MIFs and MRRs, the former have a much larger impact on systems costs. However, even the costs of MIFs represent only a slight increment at a system level. The cost effect of MRRs is barely noticeable. This confirms one of the hypotheses of the study: the flexibility of the power system allows for economically efficient arrangements to compensate fluctuations of demand. The cost increase under MIF constraints can be explained by two reasons. First, a MIF forces higher power outputs, which can imply lower end-of-week reservoir storages, with consequent higher opportunity of cost of water. Second, MIF also reduces the load-following capability and therefore another more expensive plant has to provide that service. This reduction in load-following capability also explains the cost increase for MRR.

Another interesting finding is the increasing marginal costs of the MIF constraints. This trend is observed on Figure 4, assuming the slope between any two cases is a good proxy for the average marginal cost, for all three water year types.

Regarding the cost allocation between thermal and hydro generation, the future cost function is responsible for the cost increase under large MIF. Thus, the thermal cost decreases with increasing MIF up to 1.0%, while the hydro generation cost grows up to 2.0% with respect to base case. This trend is observed for all water year types.

3.4.4. Finding Pareto-Efficient ECs

To identify Pareto-efficient ECs in terms of SDHA improvement and system cost increase, results are combined in Figure 5 for the normal water year. The inferior and efficient solutions become quite evident. Different ECs can for the same cost achieve different environmental improvements. For instance, all ECs involving MIF1 and MIF2 have a similar cost, very close to zero, but Q2R5 is clearly attains the best environmental performance. For a given MIF, the most demanding ramping constraint achieves lowest flashiness indexes at the same cost. Generally, a larger MIF constraint assures a better environmental performance, excepting for MIF5. Hence, only Q2R5, Q3R5, and Q4R5 are the constraints that form the Pareto-optimal frontier. Similar results were obtained for the dry and wet year types (Table 4).

For the Pareto-efficient ECs, duration curves of the flashiness index along with the natural flow regime are shown in Figure 6a, where constraint Q2R5 reduces by 50% the intensity of the flashiness for every probability. Constraint Q3R5 contributes with an additional reduction of around 10% and Q4R5 reduces the flashiness even further. For a R-B index threshold of 0.02 (which is exceeded 5% of the time in the natural flow regime), the current operation exceeds that limit about 50% of time. Constraint Q2R5 reduces exceedance time to 40%, Q3R5 to 30% and Q4R5 to 20%. Finding socioecologically meaningful thresholds remains an open question. Nevertheless, as ECs reduce the intensity of flashiness along the whole curve, the recommendation regarding which ECs are best still applies.

3.4.5. Impact of Efficient ECs on Other Reservoirs

So far three Pareto-efficient ECs have been identified. However, their impact on the flashiness has been considered only downstream of Pangue. As identified in the system diagnostic, reservoirs El Toro and Machicura are of importance as they both are the most downstream reservoir of their basin. Their R-B index is computed and displayed in Figures 6b and 6c. Clearly, the ECs applied on Pangue do not have a significant effect on Machicura: the flashiness curves of all cases follow the same shape. This is also the case of El Toro, excepting for the case of Q4R5 which intensifies its flashiness at probabilities of exceedance between 0.15 and 0.40. Consequently, only constraints Q2R5 and Q3R5 can be recommended for implementation, without harming other relevant basins.

4. Conclusions and Future Work

In this study, a framework for identification of Pareto-efficient environmental flow constraints (ECs) on hydropower operation was proposed. It comprises the use of an hourly grid-wide power dispatch model, in which ECs—in the form of maximum ramping rates (MRRs) and minimum flows (MIFs)—are imposed. Impact in terms of system-wide costs and subdaily hydrologic alteration (SDHA) are then assessed, leading to the identification of Pareto-efficient ECs.

The framework is illustrated through a case study in Chile, where an entire grid is modeled and the ECs are applied to one hydropower reservoir. The case study consisted of 25 cases of ECs, five MIFs (between 20% and 50% of the monthly median flow) by five MRRs (between 6 and 28% of the monthly median flow), which are evaluated for three water year types. Three out of the 25 evaluated cases were identified as the Pareto-efficient. Each of these three cases represents a different MIF, but they are all achieved at the most stringent MRR. While MRR have no noticeable effect on system cost, because there is enough flexibility to compensate for the plant's restrictions, MIF are more costly, as water with high opportunity cost is allocated to comply with this requirement.

As of the impact of water year type, constraining the operation is relevant especially for dry and normal years, where ECs achieve great results at improving the evaluated reservoir's flashiness. Noticeably, the grid-wide cost increase is small and consistently about 2% of the system-wide thermal cost for all water year types.

Regarding cross effects on other reservoirs, only the Pareto-efficient constraint set involving the most stringent MIF, worsens the hydrologic alteration downstream of another major reservoir. Consequently, the two smallest MIFs combined with the most stringent MRR are not only Pareto-efficient in terms of local hydrologic alteration but also harmless on other basins.

A limitation of this work is related to the lack of evidence regarding the ecological significance of subdaily indicators of hydrologic alteration, particularly possible thresholds. As future work, new pricing mechanisms to pay for cost increases due to ECs could be explored, especially in the case of high penetration of variable renewable energy, like wind and solar technologies. In addition, the modeling challenge remains to account for the impact of short-term operational constraints on the long-term value of water in the reservoirs. Finally, the relevance of subdaily flow records is emphasized.

Acknowledgments

The authors wish to thank Chile's National Commission for Scientific and Technological Research for supporting this research via the grant CONICYT/Fondecyt/11110326, CONICYT/Fondecyt/1120317 and CONICYT/Fondap/15110019. Preliminary work by Mauricio Fernández and Abel Quintero is greatly appreciated. We used streamflow and power system data freely available online at the *National Directorate for Water of Chile* [2013] and the *Power System Operator of Chile (CDEC)* [2013], respectively.

References

Baker, D. B., R. P. Richards, T. T. Loftus, and J. W. Kramer (2004), A new flashiness index: Charactersitics and applications to midwestern rivers and streams, *J. Am. Water Resour. Assoc.*, *40*(2), 503–522, doi:10.1111/j.1752-1688.2004.tb01046.x.

Bevelhimer, M. S., R. A. McManamay, and B. O'Connor (2015), Characterizing sub-daily flow regimes: Implications of hydrologic resolution on ecohydrology studies, *River Res. Appl.*, doi:10.1002/rra.2781, in press.

Biggs, B. J. F., V. I. Nikora, and T. H. Snelder (2005), Linking scales of flow variability to lotic ecosystem structure and function, *River Res. Appl.*, *21*(2–3), 283–298, doi:10.1002/rra.847.

Bruno, M. C., B. Maiolini, M. Carolli, and L. Silveri (2009), Impact of hydropeaking on hyporheic invertebrates in an Alpine stream (Trentino, Italy), *Ann. Limnol. Int. J. Limnol.*, *45*(3), 157–170, doi:10.1051/limn/2009018.

Bunn, S. E., and A. H. Arthington (2002), Basic principles and ecological consequences of altered flow regimes for aquatic biodiversity, *Environ. Manage.*, *30*(4), 492–507, doi:10.1007/s00267-002-2737-0.

Dos Santos, T. N., and A. L. Diniz (2011), A dynamic piecewise linear model for DC transmission losses in optimal scheduling problems, *IEEE Trans. Power Syst.*, *26*(2), 508–519, doi:10.1109/TPWRS.2010.2057263.

García, A., K. Jorde, E. Habit, D. Caamaño, and O. Parra (2011), Downstream environmental effects of dam operations: Changes in habitat quality for native fish species, *River Res. Appl.*, *27*(3), 312–327, doi:10.1002/rra.1358.

Haas, N. A., B. L. O'Connor, J. W. Hayse, M. S. Bevelhimer, and T. A. Endreny (2014), Analysis of daily peaking and run-of-river operations with flow variability metrics, considering subdaily to seasonal time scales, *J. Am. Water Resour. Assoc.*, *50*(6), 1622–1640, doi:10.1111/jawr.12228.

Haas, J., M.A. Olivares, and R. Palma-Behnke (2015), Grid-wide Subdaily Hydrologic Alteration due to Massive Wind Power Integration in Chile, *J. Environ. Manage.*, *154*, 183–189, doi:10.1016/j.jenvman.2015.02.017.

Halleraker, J. H., S. J. Saltveit, A. Harby, J. V. Arnekleiv, H.-P. Fjeldstad, and B. Kohler (2003), Factors influencing stranding of wild juvenile brown trout (Salmo trutta) during rapid and frequent flow decreases in an artificial stream, *River Res. Appl.*, *19*(5–6), 589–603, doi:10.1002/rra.752.

Halleraker, J. H., H. Sundt, K. T. Alfredsen, and G. Dangelmaier (2007), Application of multiscale environmental flow methodologies as tools for optimized management of a Norwegian regulated national salmon watercourse, *River Res. Appl.*, *23*(5), 493–510, doi:10.1002/rra.1000.

Harpman, D. A. (1999), Assessing the short-run economic cost of environmental constraints on hydropower operations at Glen Canyon Dam, *Land. Econ.*, *75*(3), 390–401, doi:10.2307/3147185.

Kern, J. D., G. W. Characklis, M. W. Doyle, S. Blumsack, and R. B. Whisnant (2012), Influence of deregulated electricity markets on hydropower generation and downstream flow regime, *J. Water Resour. Plann. Manage.*, *138*(4), 342–355, doi:10.1061/(ASCE)WR.1943–5452.0000183.

Kern, J. D., D. Patino-echeverri, and G. W. Characklis (2014), The impacts of wind power integration on sub-daily variation in river flows downstream of hydroelectric dams, *Environ. Sci. Technol.*, *48*(16), 9844–9851.

Kotchen, M. M. J., M. R. M. Moore, F. Lupi, and E. E. S. Rutherford (2006), Environmental constraints on hydropower: An ex post benefit-cost analysis of dam relicensing in Michigan, *Land. Econ.*, *82*(3), 384–403, doi:10.2307/27647719.

Krause, C. W., T. J. Newcomb, and D. J. Orth (2005), Thermal habitat assessment of alternative flow scenarios in a tailwater fishery, *River Res. Appl.*, *21*(6), 581–593, doi:10.1002/rra.829.

Lundquist, J. D., and D. R. Cayan (2002), Seasonal and spatial patterns in diurnal cycles in streamflow in the Western United States, *J. Hydrometeorol.*, *3*(5), 591–603, doi:10.1175/1525–7541(2002)003<0591:SASPID>2.0.CO;2.

McKinney, T., D. W. Speas, R. S. Rogers, and W. R. Persons (2001), Rainbow trout in a regulated river below Glen Canyon Dam, Arizona, following increased minimum flows and reduced discharge variability, *North Am. J. Fish. Manage.*, *21*(1), 216–222, doi:10.1577/1548–8675(2001)021<0216:RTIARR>2.0.CO;2.

Meile, T., J.-L. Boillat, and A. J. Schleiss (2010), Hydropeaking indicators for characterization of the Upper-Rhone River in Switzerland, *Aquat. Sci.*, *73*(1), 171–182, doi:10.1007/s00027-010-0154-7.

Ministry of Public Works of Chile (MOP) (2005), Modifica el Código de Aguas (Modifies the Water Code), 29 Dec 2009, *Bill 20.017*.

Moog, O. (1993), Quantification of daily peak hydropower effects on aquatic fauna and management to minimize environmental impacts, *Regul. Rivers Res. Manage.*, *8*, 5–14.

National Directorate for Water of Chile (2013), Fluviometric Stations, Santiago, Chile. [Available at http://dgasatel.mop.cl/, last accessed 22 Nov. 2013.]

National Energy Commission of Chile (CNE) (2013), Electricity Tariffing. [Available at http://www.cne.cl/tarificacion/electricidad/introduccion-a-electricidad, last accessed 29 Aug. 2013.]

Olivares, M. A. (2008), Optimal hydropower reservoir operation with environmental requirements, PhD dissertation, Coll. of Eng., Univ. of Calif., Davis.

Pereira, M., and L. Pinto (1991), Multi-stage stochastic optimization applied to energy planning, *Math. Program.*, *52*, 359–375.

Pérez-Díaz, J. I., and J. Wilhelmi (2010), Assessment of the economic impact of environmental constraints on short-term hydropower plant operation, *Energy Policy*, *38*(12), 7960–7970, doi:10.1016/j.enpol.2010.09.020.

Pérez-Díaz, J. I., R. Millán, D. García, I. Guisández, and J. R. Wilhelmi (2012), Contribution of re-regulation reservoirs considering pumping capability to environmentally friendly hydropower operation, *Energy*, *48*(1), 144–152, doi:10.1016/j.energy.2012.06.071.

Poff, N. L., and J. K. H. Zimmerman (2010), Ecological responses to altered flow regimes: A literature review to inform the science and management of environmental flows, *Freshwater Biol.*, *55*(1), 194–205, doi:10.1111/j.1365–2427.2009.02272.x.

Poff, N. L., J. D. Allan, M. B. Bain, J. R. Karr, K. L. Prestegaard, B. D. Richter, R. E. Sparks, and J. C. Stromberg (1997), The natural flow regime, *Bioscience*, *47*(11), 769–784, doi:10.2307/1313099.

Power System Operator of Chile (CDEC) (2013), Data, Statistics, and Reports, Santiago, Chile. [Available at https://www.cdec-sic.cl/est_opera_privada.php, last accessed 15 July 2013.]

Richter, B., J. Baumgartner, J. Powell, and D. Braun (1996), A method for assessing hydrologic alteration within ecosystems, *Conserv. Biol.*, *10*(4), 1163–1174, doi:10.2307/2387152.

Richter, B., J. Baumgartner, R. Wigington, and D. Braun (1997), How much water does a river need?, *Freshwater Biol.*, *37*(1), 231–249, doi:10.1046/j.1365–2427.1997.00153.x.

Saltveit, S. J., J. H. Halleraker, J. V. Arnekleiv, and A. Harby (2001), Field experiments on stranding in juvenile atlantic salmon (Salmo salar) and brown trout (Salmo trutta) during rapid flow decreases caused by hydropeaking, *Regul. Rivers Res. Manage.*, *17*(4–5), 609–622, doi:10.1002/rrr.652.

Scruton, D. A., C. J. Pennell, M. J. Robertson, L. M. N. Ollerhead, K. D. Clarke, K. Alfredsen, A. Harby, and R. S. McKinley (2005), Seasonal response of juvenile Atlantic Salmon to experimental hydropeaking power generation in Newfoundland, Canada, *North Am. J. Fish. Manage.*, *25*(3), 964–974, doi:10.1577/M04–133.1.

Shiau, J.-T., and F.-C. Wu (2013), Optimizing environmental flows for multiple reaches affected by a multipurpose reservoir system in Taiwan: Restoring natural flow regimes at multiple temporal scales, *Water Resour. Res.*, *49*, 565–584, doi:10.1029/2012WR012638.

Stott, B., J. Jardim, and O. Alsac (2009), DC power flow revisited, *IEEE Trans. Power Syst.*, *24*(3), 1290–1300, doi:10.1109/TPWRS.2009.2021235.

Suen, J.-P., and J. W. Eheart (2006), Reservoir management to balance ecosystem and human needs: Incorporating the paradigm of the ecological flow regime, *Water Resour. Res.*, *42*, W03417, doi:10.1029/2005WR004314.

The Nature Conservancy (2007), *Indicators of Hydrologic Alteration Version 7 User's Manual*, Arlington, Va.

Tuhtan, J. A., M. Noack, and S. Wieprecht (2012), Estimating stranding risk due to hydropeaking for juvenile European grayling considering river morphology, *KSCE J. Civ. Eng.*, *16*(2), 197–206, doi:10.1007/s12205-012-0002–5.

Vehanen, T., J. Jurvelius, and M. Lahti (2005), Habitat utilisation by fish community in a short-term regulated river reservoir, *Hydrobiologia*, *545*(1), 257–270, doi:10.1007/s10750-005-3318-z.

Yang, Y.-C. E., X. Cai, and E. E. Herricks (2008), Identification of hydrologic indicators related to fish diversity and abundance: A data mining approach for fish community analysis, *Water Resour. Res.*, *44*, W04412, doi:10.1029/2006WR005764.

Zimmerman, J. K. H., B. H. Letcher, K. H. Nislow, K. A. Lutz, and F. J. Magilligan (2010), Determining the effects of dams on subdaily variation in river flows at a whole-basin scale, *River Res. Appl.*, *26*(10), 1246–1260, doi:10.1002/rra.1324.